Multijoint arm control: beyond reaching

F.A. Mussa-Ivaldi[1,2], J. L. Patton[2], V. Chib[1], D. Sha[2], C. D. Mah[2], J. B. Dingwell[3]
[1]Department of Biomedical Engineering, Northwestern University, Chicago, IL, USA
[2]Sensoy Motor Performance Program, Rehabilitation Institute of Chicago, Chicago, IL USA
[3]Department of Kinesiology and Health Education, University of Texas at Austin, Austin, TX, USA

Abstract— **We present a set of recent results on the control of movements in which the hand interacts with force fields that simulate the presence of dynamical objects and of surface boundaries. These experiments exploit the possibility of using human/robot interactions for exploring if and how the smoothness is enforced by the adaptive control system. We conclude that a) subjects learn to generate smooth motion of transported objects and that b) significant exceptions to smooth motions are observed in hand movements over curved boundaries.**

Keywords— **Adaptation, Contact, Force-fields, Smoothness**

I. Introduction

One of the milestones in the study of multi-joint arm movements has been established by the observation that smoothness of movement appears to be an organizing principle for coordination [1-3]. In particular, Hogan and Flash have formulated this idea in what is known as minimum-jerk principle: in a reaching movement, the joints are coordinated in such a way that the trajectory of the hand minimizes the mean squared amplitude of the time derivative of hand acceleration, or "jerk". This organizing principle has been studied (and challenged [4]) in a number of experiments on reaching movements. However, less is known about movements that involve mechanical interactions with the environment. Here, we report some recent studies of multi-joint movements in which subjects interacted with force fields emulating dynamical objects and viscoelastic surfaces. Each of the studies evaluated to what degree smoothness of motion is enforced by the adaptive control mechanism underlying human motor behavior.

II. Controlling spring-mass objects

A question of significant importance in the control of robotic manipulation concerns the control of objects connected to the robot's end-effector via a number of unactuactuated degree of freedom [5, 6]. This is a common skill in human manipulation. When we carry a cup of coffee or a spoon, we are not only concerned with the motion of the container, but also with the stability of its contents. We have investigated how subjects control the motion of a virtual mass-spring system, connected to the handle of a planar manipulandum [7]. Subjects made straight line reaching movements to a target while holding the handle of the robotic manipulandum (Figure 1). The manipulandum was programmed to emulate interaction forces corresponding to the dynamics of a mass-on-a-spring. A visual display

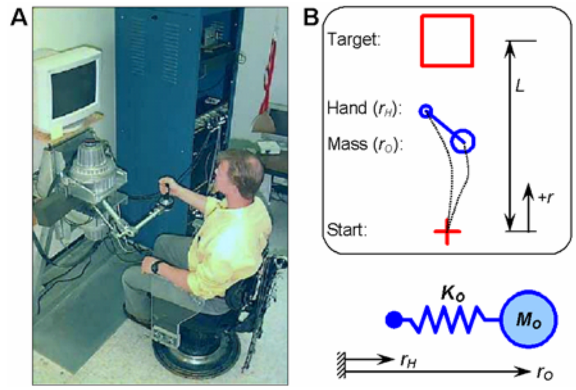

Figure 1 A. Experimental apparatus B. Simulation of a virtual spring-mass object

showed in real time the motion of the simulated object. Subjects were asked to move to, and stop the object in, a target zone. Because of the spring constant, the object tended to oscillate at a frequency of 1 Hz. All subjects displayed a learning behavior with a broad range of time constants (from 20 to 400 trials). At the end of training, all subjects were able to generate monotonic movements of the object with unimodal, bell shaped velocity profiles. To do so, the movements of the hand exhibited variable patterns, some including bimodal velocity profiles. To account for these results, we developed a mathematical model for transporting a mass-spring object to a target while optimizing a smoothness functional. This model extends the minimum jerk model for unconstrained reaching movements. A problem in this optimization arises from the increased number of boundary conditions to be satisfied when both the hand and the object are required to be at rest (zero velocity and acceleration) at the starting and ending

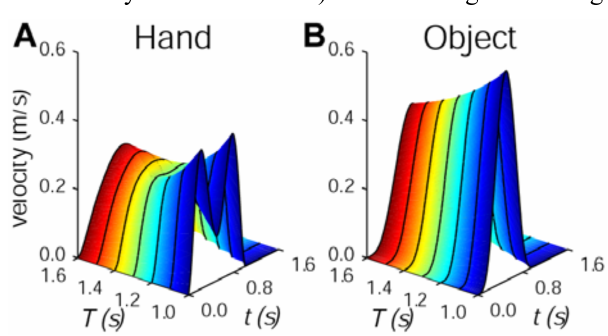

Figure 2 Model predictions. ***A***: Predicted optimal hand velocity profiles for making a 25 cm reaching movement with an object of M_O = 3 kg and K_O = 120 N/m as the desired final movement time is (T) varied. ***B***: Corresponding object velocity profiles. Object movements are always uni-phasic, whereas hand movements are uni-phasic for T > 1.34 s and bi-phasic for T < 1.34s.

positions. In the minimum-jerk model, only six such conditions must be satisfied. In contrast, when controlling the motion of a mass-spring object, the number of independent boundary condition increases to ten. Solving this problem requires a ninth order polynomial, which corresponds to optimizing the 5th derivative of position (crackle) instead of jerk. Optimization of smoothness in this generalized sense leads to predictions. In particular, there are specific combinations of task and object parameters where the model predicts that subjects will transition from the typically observed uniphasic hand motion to a biphasic hand motion (Figure 2). Such transitions are expected when, given a total distance, the required movement time decreases below a threshold. Alternatively, a transition from uniphasic to biphasic hand profile is obtained when, given a distance and movement time, the object's resonant frequency is less than a threshold value. Both transitions have been empirically observed when subjects learned to carry virtual spring/mass objects with different resonant frequencies and with different time requirements. These findings support the idea that smoothness of motion is a general principle of movement planning, which extends beyond the control of hand trajectories and applies to the motion of transported objects.

III. Disturbances vs. Boundaries

In the previous experiment, a manipulator was programmed to emulate the interaction with a transported object. This mechanical interaction is a dynamical force field that maps the state of motion of the hand into an applied force. The objects that we come in contact with in the environment can be represented as force fields. Ideally, the boundary of a rigid object has infinite stiffness. As we touch it, the hand cannot penetrate inside this boundary and, as stated by Newton's law, the boundary generates a force equal and opposite to the force that we apply. Of course, rigidity is an idealization of actual physical behavior. Nothing perfectly rigid exists, in reality. Object boundaries have impedance properties and reacts with a force to an applied motion. In many cases this motion is at all effects negligible, as for the surface of a desk. But in other cases, the motion at the boundary can be large, as when one pushes on a pillow. Given that an object boundary can be represented as a force field, the identification of such force field and the identification of an object's shape through touch requires adapting the hand motion to the surface shape. This differs quite strikingly from other known adaptive responses to perturbing force fields [8]. Earlier studies have shown that in response to a force field applied to the hand, subjects react by enforcing a smooth trajectory. To do so, they generate forces that counteract the disturbing field and that, during unexpected release of the perturbation (catch trials), lead to an after-effect opposite to the initial deflection of the movement. In contrast, if one encounters a rigid object boundary, the obvious response is to comply with the shape

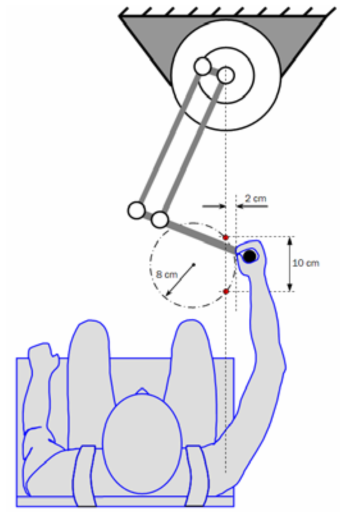

Figure 3. Apparatus for the emulation of a virtual planar boundary. The two dots on the circumference are the movement targets. The subjects did not see the outline of the circle.

of the boundary. Thus, the identification of a force field as a perturbation or as a boundary is expected to induce divergent responses: modification of the planned trajectory (object) or enforcement of the planned trajectory, with counteracting forces. These two responses would lead to opposite after-effects: deflection in the direction of the expected force field (object) or opposite to the expected force field (disturbance).

We have carried out experiments aimed at a) testing the hypothesis that such a dichotomy exist and b) determining if there is a threshold of stiffness below which a field is compensated as a disturbance and above which it is interpreted as a boundary. This analysis is based on the observation of after-effects of adaptation.

The experiments involved subjects executing trajectories while holding the same planar manipulandum of the previous study (Figure 3). In this case, the robot was programmed to render mechanically a planar virtual boundary, a disk, with variable mechanical properties. The virtual boundary was implemented by the following control law:

$$F(r) = \begin{cases} K(R-r) + B\dot{r} & r \le R \\ 0 & r > R \end{cases}$$

where r is the distance of the hand from the center of the disk, R is the radius of the disk, K and B are stiffness and viscosity constants. The center of the disk was places in front of the subject, at about 35cm from the subject's shoulder. In this experiment that radius was set to 8cm. Subjects were instructed to make reaching movements with the hand between two points on the boundary of the circle. The experiment was dividend in 5 phases, following a typical field-adaptation protocol [8]:

1) 60 movements. Unperturbed familiarization (no field).
2) 50 movements. Training with virtual surface.

3) 50 movements. Training with virtual surface and with pseudorandom catch trials, causing after-effects.
4) 50 movements. Unperturbed (washout) movement.

Each subject repeated this procedure repeated with different stiffness levels (K = 200, 400, 800, 1200, 1600, 2000 N/m).

The start and goal position, and a cursor corresponding to their hand position, were visible to the subject during testing. The boundary of the virtual surface was not visible to the subject.

To evaluate the amplitude and direction of the aftereffects, the "signed area" between the trajectory and the straight segment joining start and end target was calculated (positive = trajectory in the direction of the field; negative = trajectory opposite to the field):

$$A = \int_{y1}^{y2} x \cdot dy$$

(the start and end targets were on the y-axis, that is in the frontal direction, the x-axis was oriented rightward with respect to the subject).

We found that subjects' trajectory adaptation depended on surface stiffness (Figure 4). When a surface's stiffness exceeded a threshold value, subjects adapted by learning to produce a smooth trajectory on the surface. This was revealed by the aftereffect being in the direction of the applied forces (positive area), that is following the profile of the virtual boundary. At lower stiffness values they adapted by recovering their original kinematic pattern of movement in free space. Accordingly, the after-effects were oriented against the field, as in the force-field adaptation experiments. These responses suggest the internal representation of two distinct categories through a continuum of force fields: force disturbances and object boundaries. In the first case, the interaction forces are resisted and the trajectory is restored. In the second case, the trajectory is modified so as to reduce the interaction forces. The transition between these categories was found to take place approximately at a boundary stiffness of 1000 N/m.

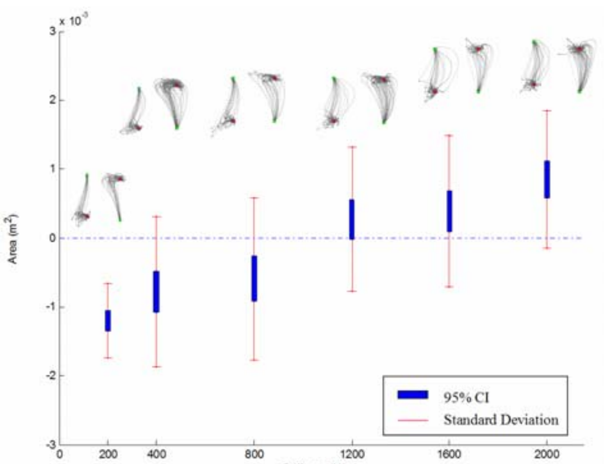

Figure 4. Signed area between the aftereffect trajectories and the straight segment joining start and end position vs. boundary stiffness of the virtual disk. Negative areas correspond to movements opposite to the force field. After effect trajectories are also plotted above the corresponding stiffness values.

IV. Constrained motions over curved surfaces

The previous experiment suggests that subjects switch from planning a smooth rectilinear motion when the boundary is soft to a curved motion when the boundary is hard. The second choice corresponds to the intention to move on the boundary, rather then resisting it. However, with a rigid boundary, smoothness can still be recovered from a constrained optimization principle. What is the trajectory corresponding to a minimum-jerk criterion over a spherical surface? The analytical answer is obtained by minimizing a functional

$$C = \int_0^{t_f} \left[\left(\frac{d^3x}{dt^3} \right)^2 + \left(\frac{d^3y}{dt^3} \right)^2 + \left(\frac{d^3z}{dt^3} \right)^2 + \lambda g(x,y,z) \right] dt,$$

where

λ is a Lagrange multiplier penalizing the undesired penetration into the constraining surface g:

$$g(x,y,z) = x^2 + y^2 + z^2 - r^2 = 0,$$

where *r* is the radius of the sphere. The resulting problem is a two-point boundary-value problem with 18 boundary conditions. While the analytical solution of this problem is complex, the outcome is geometrically quite simple: the minimum jerk trajectory takes place along the segment of *geodesic* joining start and end position. The speed along this segment follows a unimodal, symmetric temporal profile. As the identification of a geodesic line depends upon knowing the shape (i.e. the radius) of the surface, constrained smoothness can only be achieved through a learning process. Do we actually learn to move along geodesic lines if we are repeatedly moving our hand over a

Figure 5. Experimental apparatus for the generation of virtual surfaces. The subject is grasping the handle of a Phantom 3.0 (Sensable Tech.) that generates a force field corresponding to a spherical surface (not visible to the subject.

spherical surface? Do we develop a representation of the surface? To address these questions, we have investigated how subjects respond to force fields that emulate the presence of a spherical surface. We have analyzed two features: a) the trajectory of the hand and b) the contact forces against the virtual surface.

Twenty-two subjects grasped the end-effector of a robotic device (Figure 5). They were asked to make repeated movements with the eyes closed between two imagined targets. The robot rendered a virtual surface that constrained movement to a hemisphere in the center of the workspace (40 cm diameter). After the subjects practiced the movement for approximately one and half hours, we compared the change in mean contact force and in distance from the geodesic segment joining start and end positions. We also evaluated these quantities for movements to a different (test) target. Results from a single subject are shown in Figure 6. Across all subjects, we found that a) the mean contact force decreased by 20% on the training trajectories and by 35% on the test trajectories with both changes being highly significant ($p<0.0001$); b) the distance from the actual geodesic path ("geodesic distance") decreased by 11% on the training trajectory and by 13% on the test trajectory; these changes were mildly significant ($p<0.05\%$); c) the changes in contact force and in geodesic distance were statistically independent; d) while there was a reduction in geodesic distance, this variable did not converge to zero (Figure 6). In another experiment, sixteen subjects executed the same hand movements with the eyes open. In this case, the reduction of force was even larger, but the difference with the geodesic path increased, instead of decreasing, for some movements. These results suggest that subjects are forming an internal representation of the constraint, as they learn to reduce the contact forces. However, movement kinematics appeared to deviate systematically and significantly from those predicted by jerk optimization. The optimization of smoothness while reflecting the geometrical properties of Euclidean free space may not apply to movements constrained by curved surfaces.

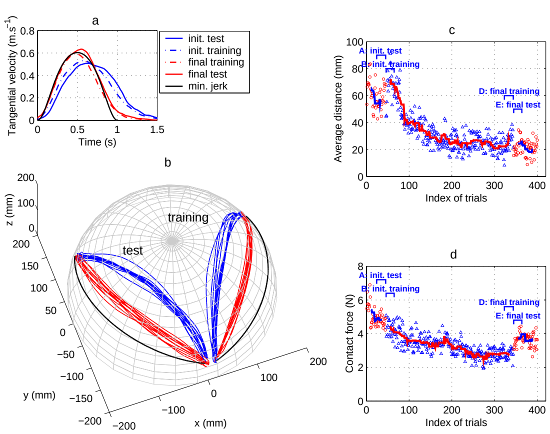

Figure 6. Training and test results for a subject's movement on the half-sphere: a) Average tangential velocity profiles of hand at four phases of experiment. Init. test: initial test on the left side . Init. training: initial part of the training phase on the right side. Final training: final part of the training phase. Final test: movements on the left side, after training on the right. Min Jerk: simulated tangential velocity profile of minimum-jerk movements. b) Hand pathways recorded during the initial (blue) and final (red) phases of training and test movements; The solid lines with the lowest z-coordinates are simulated minimum jerk solutions (i.e. geodesic paths); c) Average and mean average distance between actual and minimum-jerk trajectory; d) Average and mean average contact force against the virtual sphere; Both measures showed significant decrease with practice in both training and test movements ($p<0.001$).

V. Conclusions

Smoothness optimization appears to be an organizing principle not only for reaching movements of the hand but also for the control of objects with dynamical properties. In this case, the adaptive controller learns to generate smooth movements of the object at the expenses of more complex movements of the hand. Significant exceptions to smoothness optimization have been observed in the adaptive control of contacts with force fields emulating viscoelastic boundaries. In particular, our findings suggest that the recognition of such fields as boundaries is revealed by the transition from a smooth movement plan to a curved plan following the estimated boundary contour. This transition appears to take place at a specific threshold of stiffness.

Acknowledgment

This research was supported by NIH grant R24HD39627 and NINDS grant NS35673-05

References

[1] P. Morasso, "Spatial control of arm movements," *Experimental Brain Research*, vol. 42, pp. 223-227, 1981.

[2] N. Hogan, "An organizing principle for a class of voluntary movements," *Journal of Neuroscience*, vol. 4, pp. 2745-54, 1984.

[3] T. Flash and N. Hogan, "The coordination of arm movements: An experimentally confirmed mathematical model," *Journal of Neuroscience*, vol. 5, pp. 1688-1703, 1985.

[4] M. Kawato, Y. Maeda, Y. Uno, and R. Suzuki, "Trajectory Formation of Arm Movement by Cascade Neural Network Model Based on Minimum Torque--Change Criterion.," *Biological Cybernetics*, vol. 62, pp. 275-288, 1990.

[5] A. Bicchi and R. Sorrentino, "Dexterous manipulation through rolling," presented at Proceedings of the IEEE International Conference on Robotics and Automation, Washington, DC., 1995.

[6] K. Lynch and M. Mason, "Dynamic nonprehensile manipulation: Controllability, Planning and Experiments," *International Journal of Robotics Research*, vol. 18, pp. 64-92, 1999.

[7] J. B. Dingwell, C. D. Mah, and F. A. Mussa-Ivaldi, "Manipulating Objects With Internal Degrees of Freedom: Evidence for Model-Based Control," *Journal of Neurophysiology*, vol. 88, pp. 222-235, 2002.

[8] R. Shadmehr and F. A. Mussa-Ivaldi, "Adaptive representation of dynamics during learning of a motor task," *Journal of Neuroscience*, vol. 14, pp. 3208-3224, 1994.